Applied Physics Letters ARTICLE scitation.org/journal/apl

Magnetoelastic anisotropy of antiferromagnetic materials

Cite as: Appl. Phys. Lett. **115**, 242403 (2019); doi: 10.1063/1.5128141
Submitted: 16 September 2019 · Accepted: 29 November 2019 ·
Published Online: 9 December 2019

Ping Sheng,[1,2,a)] Yali Xie,[1,2,a)] Yuhao Bai,[3,a)] Baomin Wang,[1,2,b)] Lei Zhang,[4] Xingcheng Wen,[1,2] Huali Yang,[1,2] Xiaoyuan Chen,[1,2] Xiaoguang Li,[5] and Run-Wei Li[1,2,6,b)]

AFFILIATIONS

[1]CAS Key Laboratory of Magnetic Materials and Devices, Ningbo Institute of Materials Technology and Engineering, Chinese Academy of Sciences, Ningbo 315201, People's Republic of China
[2]Key Laboratory of Magnetic Materials and Application Technology, Ningbo Institute of Materials Technology and Engineering, Chinese Academy of Sciences, Ningbo 315201, People's Republic of China
[3]College of Physics and Electronic Information, Shanxi Normal University, Linfen 041004, People's Republic of China
[4]High Magnetic Field Laboratory, Chinese Academy of Sciences, Hefei 230031, People's Republic of China
[5]Hefei National Laboratory for Physical Sciences at the Microscale and Department of Physics, University of Science and Technology of China, Hefei 230026, People's Republic of China
[6]Center of Materials Science and Optoelectronics Engineering, University of Chinese Academy of Sciences, Beijing 100049, People's Republic of China

[a)]**Contributions:** P. Sheng, Y. Xie, and Y. Bai contributed equally to this work.
[b)]**Authors to whom correspondence should be addressed:** wangbaomin@nimte.ac.cn and runweili@nimte.ac.cn

ABSTRACT

Antiferromagnetic (AFM) materials are of great interest for spintronics. Here, we report the magnetoelastic anisotropy of an AFM IrMn thin film. An exchange-biased CoFeB/IrMn bilayer was used to obtain a single domain of the AFM thin film, and the magnetic moment arrangement of the AFM layer was deduced from the magnetic hysteresis loop of the pinned FM layer. A uniaxial compressive stress is applied on the thin film through changing the temperature due to the anisotropic thermal expansion of the polyvinylidene fluoride (PVDF) substrate. Both experimental results and theoretical calculations show that the direction of IrMn magnetic moment can be changed when a compressive stress is applied and the direction of IrMn AFM moment rotates about 10° under 2.26 GPa compressive stress. These results provide important information for the practical application of flexible spintronics based on AFM spintronic devices.

Magnetoelastic anisotropy in magnetic materials can be induced by the mechanical stresses due to the magnetoelastic coupling.[1–4] Recently, many works have been devoted to studying magnetoelastic anisotropy in ferromagnetic (FM) materials such as CoFeB and FeGa films.[5–10] Generally, the applied stresses will change the direction of easy magnetic axes, which determine the magnetization orientation of FM films. For instance, when compressive stress is applied on positive magnetostrictive materials, the magnetization orientation will be changed from the original direction to the direction away from compressive stress. Spintronic devices, such as spin valves, are dependent on the relative magnetization direction between two neighboring FM films to determine the device performance.[11–13] The antiferromagnetic (AFM) layer was considered to only play a static supporting role in enhancing the magnetic hardness of the FM layer through the exchange bias effect previously.[14] Recently, AFM materials have received extensive attention due to the increased application potential in the so-called AFM spintronics,[15–17] which utilize the properties of AFM materials to affect the performance of devices. Studying the magnetoelastic anisotropy in AFM materials, which determines the magnetization direction in the pinned magnetic reference layer and high/low resistance states in AFM spintronic devices, respectively, thus is an important topic for both fundamental research and potential practical applications.[15,18,19] When stress was applied in AFM materials, we are not sure whether the states of AFM moment are away from stress, which is defined as status A, or unchanged compared with the original direction, which is defined as status B [Fig. 1(a)]. Very recently, by using ferroelastic strain from piezoelectric materials, the electric field has been used to control the magnetic moment arrangement in several AFM thin films.[19,20] The theoretical study also indicates that strain can be exploited for the control of Néel vectors in Mn-based AFM materials.[21] However, an AFM

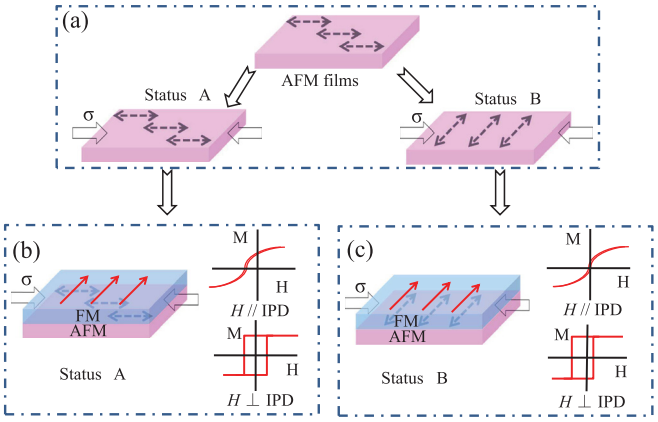

FIG. 1. (a) The schematic diagram of magnetic moment rotation in an antiferromagnetic film. The simple diagram of the exchange bias structure and the corresponding hysteresis loop parallel and perpendicular to the IPD with the external stress applied parallel to the IPD, while the direction of the AFM magnetic moment is rotated (b) and remains unchanged (c) (the red arrow represents the direction of the FM magnetic moment, and the black arrow represents the direction of the AFM magnetic moment).

thin film usually contains many different AFM domains,[22,23] which makes it difficult to explore the change of the magnetic moment arrangement of the AFM state under applied stress.

In an exchange-biased system, a single domain of the AFM state can be obtained through the interfacial exchange coupling between FM and the adjacent AFM materials.[24,25] Furthermore, the value of H_{eb} depends on the angle between the external measuring magnetic field and the pinning direction, which infers to the magnetic moment direction of the AFM layer.[26–30] When the magnetization direction of AFM material is changed, the direction of the adjacent FM layer will also be changed,[31,32] demonstrating that the change in the direction of AFM moment can be detected from the angular dependence of H_{eb}.

In this work, we designed an experiment to study the magnetoelastic anisotropy of AFM IrMn in exchange-biased FM/AFM bilayers (Fig. 1). The typical square axis loop with H_{eb} and the hard loop without H_{eb} can be obtained from exchange-biased FM/AFM bilayers without external stress. When compressive stress was applied along the initial pinning direction (IPD), the magnetization direction of positive magnetostrictive materials such as CoFeB will change to the direction away from compressive stress because of the magnetoelastic anisotropy. According to the classical exchange bias model,[25] if the direction of AFM magnetic moment remains unchanged, from the hysteresis loops parallel and perpendicular to the IPD shown in Fig. 1(b), it is found that the hard axis loop with H_{eb} and the square loop without H_{eb} can be obtained when the measuring magnetic field H is parallel and perpendicular to the IPD, respectively. In contrast, if the direction of AFM magnetic moment is changed like that in status B [Fig. 1(c)], the hard axis loop without H_{eb} can be obtained with H along the IPD while the square hysteresis loop with H_{eb} can be obtained when H is perpendicular to the IPD. Thus, the magnetoelastic anisotropy in the AFM IrMn thin film can be figured out by investigating the properties of the adjacent FM CoFeB layer in the CoFeB/IrMn system. Our results show that the direction of IrMn magnetic moment can be changed when a compressive stress is applied along the IPD and the direction of IrMn AFM moment rotates about 10° under 2.26 GPa compressive stress.

Ta(2 nm)/CoFeB(10 nm)/IrMn(30 nm)/Ta(4 nm) multilayer films were deposited on 50 μm thick polyvinylidene fluoride (PVDF) and Si substrates by dc magnetron sputtering with a base pressure below 5×10^{-8} Torr at room temperature, as schematically illustrated in Fig. 2(a). During deposition, a magnetic field $H_{growth} = 800$ Oe, which was provided by a permanent magnet, was applied along the x direction of PVDF to induce a magnetic easy axis and exchange coupling at the FM/AFM interface [Fig. 2(a)]. The bottom Ta seeding layers were employed to reduce the roughness of flexible substrates and induce the (111) texture growth of IrMn. The samples were protected from oxidation by the Ta capping layers. A quantum design superconducting quantum interference device-vibrating sample magnetometer (SQUID-VSM) was employed to measure the magnetic hysteresis loops for the CoFeB/IrMn heterostructures in the temperature range from 200 to 300 K with an interval of 20 K at various in-plane magnetic field orientations, θ, with respect to the initial direction of the EB field (x direction). The magnetic field orientation dependence of hysteresis loops was determined using a quantum design superconducting quantum interference device (SQUID). The temperature dependence of deformation in PVDF was obtained by using a Thermomechanical analyzer (TMA).

Figure 2(b) shows the hysteresis loops parallel ($\theta = 0°$) and perpendicular ($\theta = 90°$) to the IPD of the CoFeB(10 nm)/IrMn(30 nm) exchange bilayers deposited on PVDF substrates at room temperature. The EB field, H_{eb}, achieves maximum at $\theta = 0°$ and vanishes at $\theta = 90°$, indicating that the magnetic moment arrangement of the IrMn film was merged into one magnetic domain and the initial magnetic moment direction of IrMn is along the IPD that is parallel to the x direction. The square magnetic hysteresis loop becomes slanted as θ is increased from 0 to 90°, demonstrating that the magnetic easy axis of CoFeB is along the IPD that is parallel to the x direction. In order to study the temperature dependence of the AFM moment direction in

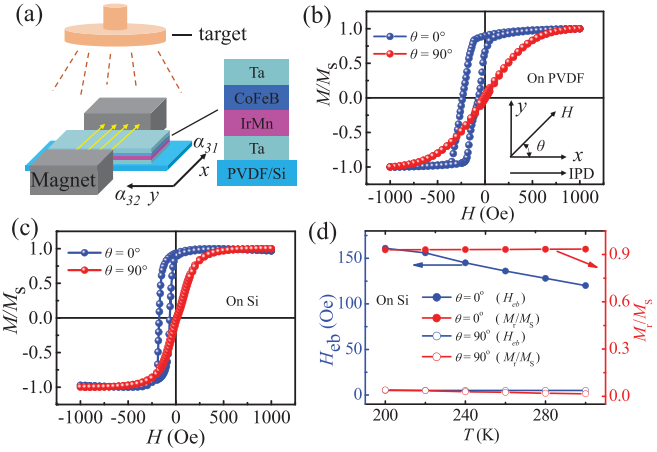

FIG. 2. (a) An illustrative drawing of the experimental setup for sample fabrication during the depositing process. (b) The hysteresis loops measured at $\theta = 0$ and 90° for the CoFeB(10 nm)/IrMn(30 nm) exchange bilayers deposited on PVDF at room temperature. (c) The hysteresis loops measured at $\theta = 0$ and 90° for the CoFeB(10 nm)/IrMn(30 nm) exchange bilayers deposited on the Si substrate at room temperature. (d) The temperature dependence of M_r/M_S and H_{eb} at $\theta = 0$ and 90°.

IrMn, a CoFeB/IrMn bilayer was deposited on the Si substrate under the same growth conditions with those of the flexible PVDF substrate as the reference sample. Figure 2(c) shows the hysteresis loops parallel and perpendicular to the IPD of the CoFeB(10 nm)/IrMn(30 nm) exchange bilayers deposited on the Si substrate at room temperature, which is similar to those observed in Fig. 2(b). The hysteresis loops with the magnetic field applied parallel and perpendicular to the IPD were also measured in the temperature range from 200 to 300 K with an interval of 20 K (not shown). The temperature dependent M_r/M_s and H_{eb} obtained both along the x and y directions are shown in Fig. 2(d). When H is along the x direction, that is, $\theta = 0°$, the value of M_r/M_s is almost unchanged (0.93) with the temperature increasing from 200 to 300 K. Similarly, M_r/M_s also remains unchanged (0.03) at $\theta = 90°$. Correspondingly, the magnetic moment direction of CoFeB is always along the IPD, indicating that the magnetic moment direction of CoFeB cannot be rotated by changing the temperature in the temperature range from 200 to 300 K. Meanwhile, the value of H_{eb} at $\theta = 0°$ decreased from 160 to 120 Oe, which is consistent with the result of the temperature effect on H_{eb}.[33] As mentioned in Fig. 2, the value of H_{eb} is zero when the measuring magnetic field is perpendicular to the AFM moment direction. Thus, the temperature dependent H_{eb} obtained at $\theta = 90°$ was used to detect the rotation of the AFM moment direction. As can be seen from Fig. 2(d), when the temperature is increased from 200 to 300 K, the value of H_{eb} at $\theta = 90°$ remains about zero, demonstrating that the temperature cannot rotate the direction of IrMn magnetic moment.

PVDF has an anisotropic thermal expansion coefficient, which can apply uniaxial stress on CoFeB/IrMn by changing the temperature of the PVDF substrate. In order to determine the value of applied stress, we define α_{31} as the thermal expansion coefficients along x and α_{32} as the thermal expansion coefficients along y directions, respectively. The thermal expansion coefficient α can be expressed as

$$\alpha = \frac{1}{L_0} \times \frac{\Delta L}{\Delta T}, \tag{1}$$

where ΔL is the change of the length when the temperature change is ΔT and L_0 is the original length of PVDF. The temperature dependent deformation is shown in Fig. 3(a). By calculating the slope of the curve, the thermal expansion coefficient is deduced to be $\alpha_{31} = 150$ ppm/K and $\alpha_{32} = 23.2$ ppm/K in the temperature range of 200–300 K. That is, when the temperature decreases below 300 K, a large anisotropic compress stress will be generated in the PVDF substrate along the x direction, which can be effectively transferred to the EB bilayers grown on it, as schematically shown in Fig. 3(b). The stress σ is estimated by

$$\sigma = \varepsilon * E_f/(1 - \upsilon^2), \tag{2}$$

where $\varepsilon = (\alpha_{31} - \alpha_{32}) \times \Delta T$, E_f is the Young's modulus of the IrMn, and υ is the Poisson ratio of the IrMn;[34] the calculated stress at different temperatures is shown in Table I.

TABLE I. The calculated stress generated in the PVDF substrate at different temperatures.

T(K)	200	220	240	260	280	300
σ(GPa)	2.26	1.81	1.35	0.90	0.45	0

Figure 4(a) shows the hysteresis loops of the CoFeB/IrMn bilayer grown on PVDF measured with H along the x direction ($\theta = 0°$) in the stress range of 0 to 2.26 GPa. The magnetic hysteresis loop becomes slanted as the stress is increased. On the other hand, the magnetic hysteresis loop along the y direction ($\theta = 90°$) becomes square and H_{eb} can be obtained as the stress is applied [Fig. 4(b)]. These results are different from that observed in the CoFeB/IrMn bilayer on the Si substrate [Fig. 2(d)], indicating that the change in M/M_s and H_{eb} is due to magnetoelastic anisotropy induced by the large anisotropic thermal expansion of the PVDF substrate. Figure 4(c) displays the stress dependence of M_r/M_s in the CoFeB/IrMn bilayer at $\theta = 0$ and 90°. When the applied stress was increased from 0 to 2.26 GPa, the M_r/M_s at $\theta = 0$ and 90° are decreased from 0.90 to 0.56 and increased from 0.04 to 0.91, respectively, indicating that the easy magnetic axis is switched from the x to y directions and the magnetic moment direction of CoFeB is along the y direction under 2.26 GPa stress. Figure 4(d) displays the stress dependence of H_{eb} in the CoFeB/IrMn bilayer at $\theta = 90°$. H_{eb} is zero without applying stress and increases to 25 Oe at 2.26 GPa, demonstrating that the induced

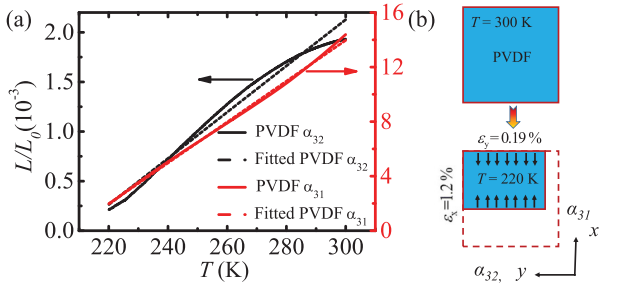

FIG. 3. (a) The temperature dependence of PVDF deformation along x and y directions. (b) The schematic diagram of PVDF at 300 K and 220 K, respectively.

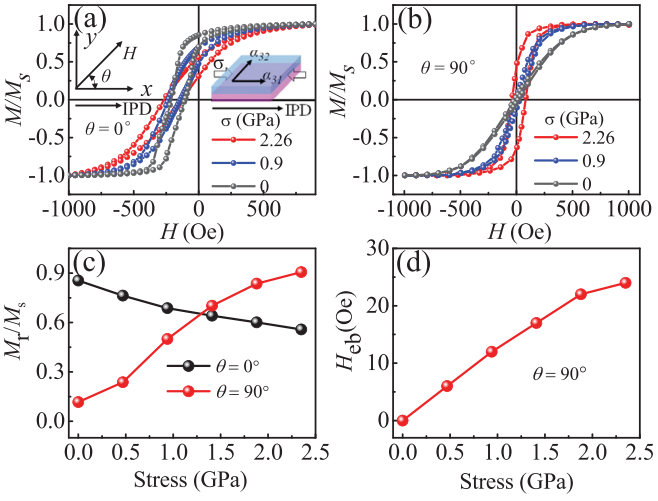

FIG. 4. Typical hysteresis loops under different stress ranges measured at $\theta = 0°$ (a) and $\theta = 90°$ (b) for the CoFeB/IrMn bilayers deposited on PVDF with the IPD set along the X direction. (c) Temperature dependence of M_r/M_s measured at $\theta = 0$ and 90°. (d) Temperature dependence of H_{eb} measured at $\theta = 90°$.

compressive stress in the IrMn film, which comes from the anisotropic thermal expansion below 300 K, can lead to the rotation of the IrMn moment.

In order to know the rotated angle (α) of IrMn moments under stress, we measured the magnetic field orientation dependence of hysteresis loops in the CoFeB/IrMn bilayer under 0 and 2.26 GPa stress. The angle dependence of H_{eb} obtained from these hysteresis loops is shown in Fig. 5(a). H_{eb} achieves zero at $\theta = 90$ and 270°, while it achieves the local maximum at 0 and 180° without applying stress on the IrMn layer. It can be nicely fitted by using the following equation:

$$H_{EB}(\theta) = \sum_{n=\text{odd}} b_n \cos n(\theta + \alpha), \tag{3}$$

where n is a positive integer and b_n is a constant.[29] As a result, $\alpha = 0$ is obtained. On the other hand, when a compressive stress of 2.26 GPa was applied on the sample along the x direction, H_{eb} achieves zero at $\theta = 80$ and 260°, while it achieves the local maximum at 170 and 350°. It can be nicely fitted with the parameters $\alpha = 10°$. As mentioned before, the change of the AFM moment direction can be detected from the angular dependence of H_{eb}; this kind of behavior indicates that 2.26 GPa compressive stress will rotate IrMn moment about 10° and positive magnetoelastic anisotropy exists in AFM IrMn thin films, as schematically shown in Fig. 5(b).

To further confirm the relationship between the AFM moment direction and the angular dependence of H_{eb}, a theoretical analysis is conducted. Considering the uniaxial anisotropy energy K_U, the exchange anisotropy energy K_E, and the Zeeman energy, the free energy per unit area of the bilayers can be written as

$$E = K_U \sin^2\theta_F - K_E \cos(\alpha - \theta_F) - HM\cos(\theta - \theta_F), \tag{4}$$

where θ_F is the angle of the ferromagnetic magnetization M along the x axis. The angle α is the pinning angle representing the direction of AFM magnetic moment along the x axis. Based on the principle of minimal energy and the coherent rotation model,[35] the hysteresis loops at different directions of the external field (θ is changed from 0 to 360°) can be obtained and the angular dependence of H_{eb} can also be inferred from these loops correspondingly. Some selected calculated hysteresis loops in different directions of the external field (θ is changed from 0 to 90°) with $\alpha = 0$ and $\alpha = 10°$ are shown in Figs. 5(c) and 5(d), respectively. For $\alpha = 0$, the square magnetic hysteresis loop becomes slanted as θ is varied from 0 to 90°. H_{eb} at $\theta = 90°$ is equal to zero, and M_r/M_s at $\theta = 0$ and 90° are 1 and 0, respectively, indicating that the easy magnetic axes of FM and AFM are collinear to each other and both of them are parallel to x directions. However, for $\alpha = 10°$, the magnetic hysteresis loop at $\theta = 0$ also becomes slanted, and H_{eb} as well as M_r/M_s at $\theta = 90°$ is not equal to zero. Additionally, the calculated angular dependence of H_{eb} inferred from these calculated hysteresis loops is consistent with the experimental results as shown in Fig. 5(a), which also demonstrates that our analyses on the arrangement of FM and AFM magnetic moments for the bilayers with and without stress are reasonable.

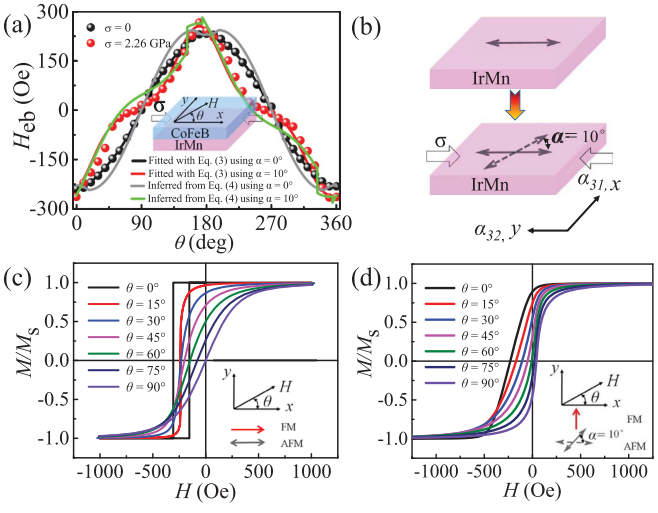

FIG. 5. (a) The angular dependence of H_{eb} measured without (black point) and with (red point) stress for the CoFeB/IrMn bilayers. (b) The schematic diagram of IrMn magnetic moment without and with stress. Some selected calculated hysteresis loops at different directions of the external field (θ is changed from 0 to 90°) (c) with $\alpha = 0°$ and (d) with $\alpha = 10°$.

In summary, we have studied the magnetoelastic anisotropy of the AFM IrMn thin film by measuring the properties of the adjacent FM CoFeB layer in the exchange-biased CoFeB/IrMn bilayers on the PVDF substrate. An exchange-biased CoFeB/IrMn bilayer was used to obtain a single domain of the AFM thin film. The magnetic hysteresis loop of the pinned FM CoFeB layer was measured to deduce the magnetic moment arrangement of the AFM IrMn layer. A uniaxial compressive stress was applied through changing the temperature of the sample due to the anisotropic thermal expansion of the PVDF substrate. Our results show that the direction of the AFM magnetic moment of IrMn will rotate when a uniaxial compressive stress is applied. From the angle dependent magnetic measurement, it can be obtained that a compressive stress of 2.26 GPa makes the direction of the IrMn AFM magnetic moment rotate about 10°. Theoretical calculations further confirmed our experimental results. This study provides important information for the practical application of flexible spintronics based on AFM spintronic devices.

This work was supported by the National Key Technologies R&D Program of China (Nos. 2016YFA0201102 and 2016YFA0300103), the National Natural Science Foundation of China (Nos. 51571208, 51871232, 51871233, 51525103, and 51931011), the Youth Innovation Promotion Association of the Chinese Academy of Sciences (Nos. 2016270 and 2019299), the Ningbo Science and Technology Bureau (No. 2018B10060), and the Ningbo Science and Technology Innovation Team (No. 2015B11001).

REFERENCES

[1]R. M. Bozorth, *Ferromagnetism* (IEEE Press,1993).
[2]E. W. Lee, Rep. Prog. Phys. **18**, 184 (1955).
[3]E. Kneller, *Ferromagnetismus* (Springer, 1962).
[4]D. C. Jiles and D. L. Atherton, J. Phys. D: Appl. Phys. **17**, 1265 (1984).
[5]G. H. Dai, Q. F. Zhan, Y. W. Liu, H. L. Yang, X. S. Zhang, B. Chen, and R. W. Li, Appl. Phys. Lett. **100**, 122407 (2012).
[6]Z. H. Tang, B. M. Wang, H. L. Yang, X. Y. Xu, Y. W. Liu, D. D. Sun, L. X. Xia, Q. F. Zhan, B. Chen, M. H. Tang, Y. C. Zhou, J. L. Wang, and R. W. Li, Appl. Phys. Lett. **105**, 103504 (2014).
[7]Y. W. Liu, B. M. Wang, Q. F. Zhan, Z. H. Tang, H. L. Yang, G. Liu, Z. H. Zuo, X. S. Zhang, X. L. Xie, X. J. Zhu, B. Chen, J. L. Wang, and R.-W. Li, Sci. Rep. **4**, 6615 (2014).

[8]X. C. Wen, B. M. Wang, P. Sheng, S. Hu, H. L. Yang, K. Pei, Q. F. Zhan, W. X. Xia, H. Xu, and R. W. Li, Appl. Phys. Lett. **111**, 142403 (2017).
[9]X. Y. Qiao, X. C. Wen, B. M. Wang, Y. H. Bai, Q. F. Zhan, X. H. Xu, and R. W. Li, Appl. Phys. Lett. **111**, 132405 (2017).
[10]X. Y. Qiao, B. M. Wang, Z. H. Tang, Y. Shen, H. L. Yang, J. L. Wang, Q. F. Zhan, S. N. Mao, X. H. Xu, and R. W. Li, AIP Adv. **6**, 056106 (2016).
[11]G. A. Prinz, Science **282**, 1660 (1998).
[12]M. N. Baibich, J. M. Broto, A. Fert, F. Nguyen Van Dau, F. Petroff, P. Etienne, G. Creuzet, A. Friederich, and J. Chazelas, Phys. Rev. Lett. **61**, 2472 (1988).
[13]G. Binasch, P. Grünberg, F. Saurenbach, and W. Zinn, Phys. Rev. B **39**, 4828 (1989).
[14]C. Chappert, A. Fert, and F. Nguyen Van Dau, Nat. Mater. **6**, 813 (2007).
[15]A. H. MacDonald and M. Tsoi, Philos. Trans. R. Soc., A **369**, 3098 (2011).
[16]T. Jungwirth, X. Marti, P. Wadley, and J. Wunderlich, Nat. Nanotechnol. **11**, 231 (2016).
[17]B. G. Park, J. Wunderlich, X. Marti, V. Holy, Y. Kurosaki, M. Yamada, H. Yamamoto, A. Nishide, J. Hayakawa, H. Takahashi, A. B. Shick, and T. Jungwirth, Nat. Mater. **10**, 347 (2011).
[18]X. Marti, I. Fina, C. Frontera, J. Liu, P. Wadley, Q. He, R. J. Paull, J. D. Clarkson, J. Kudrnovský, I. Turek, J. Kuneš, D. Yi, J.-H. Chu, C. T. Nelson, L. You, E. Arenholz, S. Salahuddin, J. Fontcuberta, T. Jungwirth, and R. Ramesh, Nat. Mater. **13**, 367 (2014).
[19]H. Yan, Z. X. Feng, S. L. Shang, X. N. Wang, Z. X. Hu, J. H. Wang, Z. W. Zhu, H. Wang, Z. H. Chen, H. Hua, W. K. Lu, J. M. Wang, P. X. Qin, H. X. Guo, X. R. Zhou, Z. G. Leng, Z. K. Liu, C. B. Jiang, M. Coey, and Z. Q. Liu, Nat. Nanotechnol. **14**, 131 (2019).
[20]X. Z. Chen, X. F. Zhou, R. Cheng, C. Song, J. Zhang, Y. C. Wu, Y. Ba, H. B. Li, Y. M. Sun, Y. F. You, Y. G. Zhao, and F. Pan, Nat. Mater. **18**, 931 (2019).
[21]I. J. Park, T. Lee, P. Das, B. Debnath, G. P. Carman, and R. K. Lake, Appl. Phys. Lett. **114**, 142403 (2019).
[22]E. Y. Ma, Y. T. Cui, K. Ueda, S. J. Tang, K. Chen, N. Tamura, P. M. Wu, J. Fujioka, Y. Tokura, and Z. X. Shen, Science **350**, 538 (2015).
[23]M. J. Grzybowski, P. Wadley, K. W. Edmonds, R. Beardsley, V. Hills, R. P. Campion, B. L. Gallagher, J. S. Chauhan, V. Novak, T. Jungwirth, F. Maccherozzi, and S. S. Dhesi, Phys. Rev. Lett. **118**, 057701 (2017).
[24]W. H. Meiklejohn and C. P. Bean, Phys. Rev. **102**, 1413 (1956).
[25]J. Nogues and I. K. Schuller, J. Magn. Magn. Mater. **192**, 203 (1999).
[26]J. Yang, S. Cardoso, P. P. Freitas, T. Devolder, and M. Ruehrig, J. Appl. Phys. **109**, 07D704 (2011).
[27]Z. Z. Guo, Solid State Commun. **151**, 116 (2011).
[28]X. L. Tang, H. Su, H. W. Zhang, Y. L. Jing, and Z. Y. Zhong, J. Appl. Phys. **112**, 073916 (2012).
[29]R. B. da Silva, M. A. Corrêa, E. F. Silva, T. J. A. Mori, R. D. Della Pace, R. Dutra, A. D. C. Viegas, F. Bohn, and R. L. Sommer, Appl. Phys. Lett. **104**, 102405 (2014).
[30]T. Ambrose, R. L. Sommer, and C. L. Chien, Phys. Rev. B **56**, 83 (1997).
[31]K. O'Grady, L. E. Fernandez-Outon, and G. Vallejo-Fernandez, J. Magn. Magn. Mater. **322**, 883 (2010).
[32]G. Vallejo-Fernandez, L. E. Fernandez-Outon, and K. O'Grady, J. Phys. D: Appl. Phys. **41**, 112001 (2008).
[33]W. Zhang and K. M. Krishnan, J. Appl. Phys. **115**, 17D714 (2014).
[34]N. Lei, S. Park, P. Lecoeur, D. Ravelosona, C. Chappert, O. Stelmakhovych, and V. Holy, Phys. Rev. B **84**, 012404 (2011).
[35]J. Camarero, J. Sort, A. Hoffmann, J. M. Garcia-Martin, and B. Dieny, Phys. Rev. Lett. **95**, 057204 (2005).